Carbon dioxide exchange of a pepperweed (*Lepidium latifolium* L.) infestation: How do flowering and mowing affect canopy photosynthesis and autotrophic respiration?

O. Sonnentag,[1,2] M. Detto,[1] B. R. K. Runkle,[3,4] Y. A. Teh,[1,5] W. L. Silver,[1] M. Kelly,[1] and D. D. Baldocchi[1]

Received 16 August 2010; revised 2 November 2010; accepted 16 November 2010; published 25 February 2011.

[1] The net ecosystem carbon dioxide (CO_2) exchange of invasive plant infestations, such as perennial pepperweed (*Lepidium latifolium* L.), is not well understood. A characteristic feature of pepperweed's phenological cycle is its small white flowers during secondary inflorescence. Pepperweed flowering causes uniform reflectance over the visible range of the electromagnetic spectrum, thus decreasing the amount of energy absorbed by the canopy and available for photosynthesis. Little is known about how pepperweed flowering and control measures such as mowing affect canopy photosynthesis and autotrophic respiration (F_{AR}) and thus ecosystem respiration. To examine this question, we analyzed CO_2 flux measurements made with eddy covariance over a pepperweed infestation in California, covering three growing seasons. Unmowed pepperweed caused the site to be almost CO_2 neutral (2007: −28 g C m^{-2} $period^{-1}$) or a net source (2009: 129 g C m^{-2} $period^{-1}$), mostly because of reduced maximum photosynthetic capacity by 13 (2007) and 17 μmol m^{-2} s^{-1} (2009) due to flowering during the plant's prime photosynthetic period. Reference F_{AR} at 10°C was reduced by 2 μmol m^{-2} s^{-1} in 2007 and 2009. Mowing during early flowering reversed the attenuating effects of pepperweed flowering, causing the site to act as a net CO_2 sink (2008: −174 g C m^{-2} $period^{-1}$) mainly due to prolonged photosynthetic CO_2 uptake over the plant's early vegetative growth phase. Our results highlight the tight link between pepperweed's prominent key phenological phase and applied control measures, which together exert dominant control over the infestation's CO_2 source-sink strength.

Citation: Sonnentag, O., M. Detto, B. R. K. Runkle, Y. A. Teh, W. L. Silver, M. Kelly, and D. D. Baldocchi (2011), Carbon dioxide exchange of a pepperweed (*Lepidium latifolium* L.) infestation: How do flowering and mowing affect canopy photosynthesis and autotrophic respiration?, *J. Geophys. Res.*, *116*, G01021, doi:10.1029/2010JG001522.

1. Introduction

[2] Biological invasions are a critical issue regarding the structure, functioning, and services of terrestrial ecosystems [*Mack et al.*, 2000; *Reichard and Hamilton*, 1997]. Plant invasions can alter their major biogeochemical cycles, soil chemical and physical properties, the type, frequency, and intensity of disturbances, and gas and energy exchanges [*Blank and Young*, 2004; *D'Antonio and Vitousek*, 1992; *Ehrenfeld*, 2003; *Potts et al.*, 2008]. Functional traits that contribute to the competitive superiority of invasive over native plants include better resource acquisition capabilities (e.g., nitrogen (N) fixation, higher root biomass, specific leaf area and leaf N content), higher resource use efficiencies, and better reproduction and dispersal strategies [*Drenovsky et al.*, 2008; *Funk and Vitousek*, 2007]. In addition, phenology, i.e., the timing of periodic events in plants' life cycles, has been identified as potentially crucial for understanding the success of invasive over native plants [*Godoy et al.*, 2009; *Wolkovich and Cleland*, 2010].

[3] The study of invasive plants has mainly focused on their biology, geographic distributions, infestation dynamics, and control measures from a land use and ecosystem restoration perspective [*Drenovsky et al.*, 2008; *Ostertag et al.*, 2009; *Renz and Blank*, 2004; *Young et al.*, 1998]. In contrast, ecosystem gas and energy exchanges of invasive plant infestations and their response to land use practices, especially in relation to invasive plant phenology, have been the subject of fewer studies [*Hunt et al.*, 2002; *Koteen*, 2009; *Potts et al.*, 2008; *Prater et al.*, 2006]. For example, using data from static chamber measurements, *Potts et al.* [2008] showed that

[1]Department of Environmental Science, Policy, and Management, University of California, Berkeley, California, USA.
[2]Department of Organismic and Evolutionary Biology, Harvard University, Cambridge, Massachusetts, USA.
[3]Department of Civil and Environmental Engineering, University of California, Berkeley, California, USA.
[4]Department of Soil Science, University of Hamburg, Hamburg, Germany.
[5]School of Geography and Geosciences, University of St. Andrews, St. Andrews, UK.

0148-0227/11/2010JG001522

the presence of invasive, deeply rooted perennial artichoke thistle (*Cynara cardunculus*) in a coastal California grassland caused increased aboveground biomass and associated increases in growing season photosynthetic carbon dioxide (CO_2) uptake and evapotranspiration (ET), and enhanced litter quality and quantity compared to a noninfested grassland, thus intensifying the carbon, water and nutrient cycles of these ecosystems.

[4] Eddy covariance is a widely used micrometeorological technique to measure the fluxes of carbon, water and energy across the interface between the soil-vegetation system and the atmosphere [*Baldocchi*, 2008]. The net ecosystem CO_2 exchange (F_C) measured with eddy covariance represents the small difference between ecosystem CO_2 uptake through canopy photosynthesis (F_A) and CO_2 release through ecosystem respiration (F_{ER}; $F_C = F_{ER}$-F_A), itself the sum of heterotrophic (F_{HR}) and autotrophic respiration (F_{AR}).

[5] Perennial pepperweed (*Lepidium latifolium* L.) is an aggressive invasive weed that is established throughout the western United States and parts of Canada including Alberta and British Columbia [*Francis and Warwick*, 2007]. Pepperweed was introduced to North America from southeastern Europe and western Asia (1930s), tolerating a wide range of soils including saline and alkaline conditions, and generally occurring in dense patches as monocultures with canopies approaching 2 m in height [*Young et al.*, 1998; *Francis and Warwick*, 2007]. A combination of functional traits has been reported to contribute to pepperweed's widespread successful establishment including aggressive vegetative growth, deep rhizome penetration, and prolific bud production and reproduction by seeds [*Francis and Warwick*, 2007].

[6] The environmental and economic impacts of pepperweed have been detrimental. Infestations of pastures and hay meadows have resulted in decreased forage quality and, consequently, in unmarketable hay [*Francis and Warwick*, 2007; *Young et al.*, 1998]. Reported pepperweed control measures include burning, flooding, grazing, mowing, and herbicide application [*Renz and Blank*, 2004]. For example, spring grazing to inhibit growth and mowing is often employed in pastures to prevent seed dispersal and litter accumulation [*Young et al.*, 1998].

[7] The canopy-scale spectral characteristics of a pepperweed infestation are distinctively different from most native plants when pepperweed is flowering [*Andrew and Ustin*, 2006]. During secondary inflorescence the canopy top contains a dense arrangement of small white flowers: sepals (leaf-like structures, together forming the calyx that protects the corolla of a flower), ~1.2 × 08 mm; petals (colorful, leaf-like structures, together forming the corolla of a flower), ~2.1 × 11 mm (for more information on flower characteristics, see *Francis and Warwick* [2007]), resulting in relatively uniform reflectance across the visible part of the electromagnetic spectrum [*Andrew and Ustin*, 2006; *Young et al.*, 1998]. In the western United States, pepperweed flowers during spring and summer from mid-May to late August following germination (~late February–March) and a short early vegetative growth phase (~April to early May) [*Andrew and Ustin*, 2008; *Francis and Warwick*, 2007]. The flowering phase of pepperweed is followed by short seed maturation (~September to mid-October) and senescence phases (late October to November). Of these, pepperweed flowering warrants special attention mainly because of its prolonged duration relative to other key phenological phases (i.e., early vegetative growth, seed maturation, senescence) and its impact on the amount of energy absorbed by the canopy that is available for photosynthesis. In addition, increased understanding of invasive plant phenology in relation to functioning was identified as an important research theme in community ecology to better understand invasive plant species' success and to develop effective management strategies [*Wolkovich and Cleland*, 2010].

[8] The goal of our study was to explore the link among pepperweed flowering, a widely applied pepperweed control measure (i.e., mowing) and net ecosystem CO_2 exchange, F_C. Specifically, we sought to determine how pepperweed flowering and mowing affected F_A and F_{AR} (and thus F_{ER}) at an ecosystem scale. Ecosystem-scale understanding of the interactions between spectrally unique pepperweed flowering, mowing and F_C is a crucial first step toward understanding the complexity introduced by invasive plants and their applied control measures. To meet our goal we analyzed eddy covariance data supported by a series of environmental measurements from a pepperweed-infested pasture in California. The measurements were taken between 4 April 2007 and 30 September 2009 and cover three meteorologically similar summer growing seasons (1 May to 30 September) that differed slightly in land use practices. In 2007–2009, the site was subjected to year-round grazing by beef cattle, and in 2008, the site was additionally mowed (i.e., pepperweed was cut but not removed from the site) in mid-May (day of year (DOY) 137) during early flowering.

2. Materials and Methods

2.1. Study Site

[9] Our study site (~0.9 × ~0.4 = ~0.36 km^2) was a fenced peatland pasture on Sherman Island (latitude: 38.0367°N; longitude: 121.7540°W; elevation: 7 m below sea level) in California's Sacramento–San Joaquin River Delta (hereafter referred to as "the Delta"), about 60 km northeast of San Francisco, California, USA. The climate of the Delta is Mediterranean with dry, hot summers and wet, cool winters. Mean annual total precipitation at the site is 335 mm and mean annual air temperature is 15.1°C (1949–1999 for Antioch climate station ~10 km southwest of Sherman Island).

[10] Alteration of the Delta began in the 1850s as an outgrowth of human settlement following the California Gold Rush. Settlers drained the tidal marshes for agriculture and livestock by establishing a dense network of dikes, waterways and ditches to regulate water flow across the landscape, thus creating a total of 57 islands bounded by levees [*Healey*, 2008]. Extensive soil drainage has promoted massive land subsidence and carbon oxidation of peat, with the average ground surface level of the Delta's islands ranging 6 to 8 m below sea level [*Mount and Twiss*, 2005].

[11] The pasture is flat and bounded and dissected by land management ditches that are part of a Delta-wide drainage network to maintain an aerated root zone above the water table, typically between 0.6 and 2 m below the ground surface [*Deverel et al.*, 2007]. The upper 60 cm of the soil profile is classified by the gravimetric hydrometer method as silty or clay loam with a soil carbon content of 5–7% and 18% near the ground surface and at 55 cm, respectively [*Runkle*, 2009]. This upper mineral soil layer overlays massive peat deposits

with a thickness of >7 m [*Deverel and Rojstaczer*, 1996; *Drexler et al.*, 2009].

[12] The northern part of the pasture (~30% of the total area) was characterized by a combination of bare soil and vegetated patches of short (maximum 0.1 m) invasive annual C_3 grass (mouse barley; *Hordeum murinum* L.). In contrast, the southern part (~70% of the total area) was almost entirely infested by pepperweed, which had been growing at the site for more than 20 years (J. Mercado, land manager, personal communication, 2010). The relative biomass of pepperweed and mouse barley in the southern part changed throughout the year, as grass precedes pepperweed in its maximum coverage. Throughout the study period, the pasture was subjected to year-round grazing by beef cattle (n = ~100, i.e., ~278 km^{-2}), causing a discontinuous, open pepperweed canopy of varying height (maximum 1 m) and density over bare soil and small patches of short grass. Dry biomass samples taken at several locations in the southern part through the season indicate areas with 13–37% pepperweed by mass at DOY 89 (2009), and 47–87% pepperweed by mass at DOY 115 (2009), which immediately precedes flowering. Samples from DOY 128 and DOY 134 (2009) show pepperweed's contribution to the site's dry biomass as 92% and 89%, respectively; this relative dominance continues through the summer.

2.2. Eddy Covariance and Supporting Environmental Measurements

[13] The fluxes of CO_2 (F_C; μmol m^{-2} s^{-1}), and sensible (H; W m^{-2}) and latent heat (λE; W m^{-2}) between the pepperweed infestation and the atmosphere were obtained with the eddy covariance technique [*Baldocchi*, 2003]. A micrometeorological tower was located in the southeastern section of the pepperweed-infested southern part of the pasture within a fenced enclosure to prevent cattle from interfering with the instrumentation (see Figure 1 of *Detto et al.* [2010]). The eddy covariance system was mounted on the tower on a 3.15 m boom oriented toward the northwest, the prevailing wind direction. The tower's homogenous upwind fetch extends ~900 m over pepperweed-infested pasture. An earlier study showed that the fluxes have a source area dominated by pepperweed (see Figure 1 of *Detto et al.* [2010]).

[14] Fluctuations in longitudinal, lateral and vertical wind velocities (*u*; *v*; *w*; m s^{-1}) and speed of sound (*sos*; m s^{-1}) were measured with a sonic anemometer (Gill WindMaster Pro; Gill Instruments Ltd, Lymington, Hampshire, England). An open-path infrared gas analyzer (LI-7500; LI-COR, Lincoln, NE, USA) was used to measure molar CO_2 (ρ_{CO2}) and water vapor (ρ_{H2O}) density fluctuations (mmol m^{-3}). The high-frequency digital output from the two instruments was recorded to a computer at a scan rate of 10 Hz and stored as half-hourly block averages.

[15] In addition to eddy covariance, a suite of supporting environmental measurements was continuously made within the fenced enclosure. Precipitation (mm) was measured with a tipping bucket rain gauge (TE525; Texas Electronics Inc., Dallas, TX, USA). Water table depth (cm) was measured with a pressure transducer (PDCR 1830; GE Druck, Billerica, MA, USA) immersed in a well. Air temperature (T_{air}; °C) and relative humidity (%) were measured with an aspirated and shielded thermistor and capacitance sensor (HMP45C; Vaisala, Vantaa, Finland) mounted on the tower at a height of 2.5 m. Soil temperatures (T_{soil}; °C) were measured at depths (−50, −32, −16, −8, −4, −2 cm) with six copper-constantan thermocouples. Net radiation (R_{net}; W m^{-2}) was measured at a height of 2.8 m with a four-component net radiometer (CNR1; Kipp and Zonen, Delft, Netherlands) mounted on 2 m boom oriented to the south. Incoming and outgoing photosynthetically active radiation (PAR; PAR_{out}) was measured as photosynthetic photon flux density (PPFD; μmol m^{-2} s^{-1}) with quantum sensors (PAR-LITE; Kipp and Zonen), and PAR_{albedo} was obtained as the ratio of PAR_{out} and PAR. Ground heat flux (G; W m^{-2}) was measured at three locations using ground heat flux plates (HFP01; Hukseflux Thermal Sensors B.V., Delft, Netherlands) buried at a depth of −2 cm. All environmental measurements were logged by data loggers (CR10; Campbell Scientific, Logan, UT, USA) at 5 s intervals and recorded as half-hourly mean values.

2.3. Plant Area Index

[16] Pepperweed leaf area index (LAI) was measured at 1–3 week intervals in 2009 using the LAI-2000 Plant Canopy Analyzer (LI-COR). The measurements were made every 10 m along a 500 m, east-west oriented transect across the tower's upwind fetch, following the measurement protocol of *Sonnentag et al.* [2007]. The LAI-2000 instrument measures effective LAI by detecting blue diffuse light penetrating a canopy [*Welles and Norman*, 1991]. Effective LAI includes the contribution of all canopy elements to light interception and does not account for foliage clumping [*Chen*, 1996]. By processing the LAI-2000 raw data with the vendor's software (FV2000.exe), clumping effects were partly accounted for [*Ryu et al.*, 2010], but we did not correct our measurements for the contribution of white flowers to light interception. Thus, we refer to our LAI estimates more accurately as plant area index (PAI).

2.4. Data Handling and Processing

[17] We calculated half-hourly mean fluxes of F_C, H, and λE from sonic temperature (T_{sonic}), *u*, *v*, *w* and ρ_{CO2}, and ρ_{H2O} after applying a series of standard corrections and adjustments [*Detto et al.*, 2010], using in-house software. First, artificial spikes were removed, followed by application of a three-coordinate rotation and removal of air density fluctuations [*Detto and Katul*, 2007; *Tanner and Thurtell*, 1969; *Webb et al.*, 1980]. Special attention was paid to artificial spikes introduced by the presence of cattle in the direct vicinity of the tower, which were manually removed based on anomalously high methane fluxes and high-frequency digital photographs in which cattle was present [*Detto et al.*, 2010; D. Baldocchi et al., The trials and tribulations of measuring methane fluxes and concentrations over a peatland pasture in the Sacramento–San Joaquin River Delta of California, submitted to *Agricultural and Forest Meteorology*, 2011]. Fluctuations in T_{sonic} were calculated from fluctuations in *sos* after removing crosswind and humidity effects [*Kaimal and Gaynor*, 1991; *Schotanus et al.*, 1983]. As an indicator for eddy covariance system performance we estimated the surface energy balance closure based on half-hourly values for H, λE, R_{net} and G (with $H + \lambda E = R_{net} - G$) as 0.79, which is comparable to other sites reported in the literature [*Wilson et al.*, 2002].

[18] Net ecosystem CO_2 exchange is the small difference between two large component fluxes, i.e., canopy photosynthesis (F_A) and ecosystem respiration (F_{ER}). We use the

atmospheric sign convention so that negative F_C indicates net CO_2 uptake by the ecosystem whereas a positive F_C indicates net CO_2 loss to the atmosphere. Representative daily and seasonal totals of F_C, F_A and F_{ER} were calculated after gap filling with the neural network approach of *Papale and Valentini* [2003] and subsequent flux partitioning based on linear relationships between nighttime F_C (PAR < 4 μmol m^{-2} s^{-1}) and T_{soil} at a depth of −2 cm within 30 day mowing window. Uncertainty in seasonal totals of F_C, F_A and F_{ER} due to the gap filling and flux-partitioning process was quantified as one standard deviation for 100 data sets based on a bootstrapping technique as outlined by *Sonnentag et al.* [2010]. However, it needs to be stressed that our uncertainty estimates do not include uncertainties from random or systematic errors. Whereas the former are negligible, the latter can be the main contributors to the overall uncertainty in annual totals of F_C, F_A and F_{ER} [*Lasslop et al.*, 2010].

[19] Surface roughness length (z_{0m}; m), the height above the ground surface where mean wind speed extrapolates to zero [*Monteith and Unsworth*, 1990], is an important parameter in land surface schemes [*Garratt*, 1992]. We used z_{0m} as a proxy to describe continuous changes in the structural development of the pepperweed canopy, as z_{0m} scales with canopy height [*Shaw and Pereira*, 1982] and is also related to leaf area index [*Lindroth*, 1993; *Raupach*, 1994], one of the most important descriptors of canopy structure. We calculated half-hourly z_{0m} during near-neutral stratification (|z/L| < 0.025, where L is the Obukhov's length) and relatively high winds (u > 1 m s^{-1}) with:

$$z_{0m} = \frac{z - d_0}{\exp\left((\kappa) * u/u_*\right)} \tag{1}$$

where z is the measurement height (3.15 m), d_0 is the zero-displacement height (m), κ is the von Karman constant (0.4), u and u_* are the wind speed (m s^{-1}) and friction velocity (m s^{-1}), respectively, both obtained from half-hourly averages of sonic anemometer measurements. With $d_0 = 0.66*h$ and $z_{0m} = 0.1*h$ where h is the canopy height, we estimated z_{0m}, d_0 and h iteratively.

2.5. Analyses

[20] To assess the impact of flowering and mowing on F_A and F_{AR}, we examined the effect of flowering (treated as a factor with the levels "Flower off" versus "Flower on") in addition to the effect of measurement year (treated as a factor with the levels "2007" versus "2008" versus "2009") using nonlinear mixed-effects models [*Davidian and Giltinan*, 2003; *Pinheiro and Bates*, 2000]:

$$y_{ij} = f\left(x_{ij}, \beta, u_i\right) + e_{ij}, \tag{2}$$

where f is a nonlinear function of known vector covariates x_{ij} for the jth measurement on the ith subject (here: week), β are unknown fixed effects for a 3-by-2 factorial design (3 measurement years each with two flowering conditions) that represent the population average of each parameter, and u_i is an unknown vector of random effects that represent the deviation of each parameter of the ith subject from the population average. The prediction errors e_{ij} are considered independent, identically distributed Gaussian processes with zero mean and finite (constant) variances. Considering measurement year as a factor in equation (2) implicitly accounts for seasonal differences in meteorological and resulting environmental controls on F_A and F_{AR}. Nonlinear mixed effects have been widely applied in many fields (see application examples in the work of *Davidian and Giltinan* [2003]), however so far, this repeated-measurement approach has been rarely applied in fitting nonlinear ecophysiological response curves [e.g., *Peek et al.*, 2002; *Lin et al.*, 2008].

[21] The nonlinear mixed-effects models (equation (2)) were fitted using methods implemented in the nlme library (v3.1) [*Pinheiro and Bates*, 2000]: the maximum likelihood parameter estimation is based on the two-step alternating algorithm (penalized nonlinear least squares step and linear mixed effects step) of *Lindstrom and Bates* [1990].

[22] First, we were interested in the effect of measurement year and flowering (2007 and 2009) and flowering/mowing (2008), respectively, on the model parameters of the rectangular hyperbolic light-response function (f in equation (2)), α and A_{max}, written as:

$$F_{A,norm} = \frac{\alpha * APAR * A_{\max}}{\alpha * APAR + A_{\max}}, \tag{3}$$

where $F_{A,norm}$ is the F_A normalized by PAI, APAR is the absorbed photosynthetically active radiation (μmol m^{-2} s^{-1}), α (μmol CO_2 μmol $photon^{-1}$) is the effective quantum yield, and A_{max} (μmol m^{-2} s^{-1}) is the maximum photosynthetic capacity. Normalizing F_A by PAI removed the effect of different amounts of photosynthesizing plant material between years. In contrast to numerous other studies [e.g., *Bergeron et al.*, 2007; *Humphreys et al.*, 2006], we used APAR instead of incoming PAR in equation (3) to incorporate the effect of changes in PAR_{albedo} due to flowering, thus accounting for the effect of changes in absorbed light available for photosynthesis. We derived weekly PAI estimates through inversion of the nonlinear relationship between weekly mean z_{0m} and spring (≈early vegetative growth) and early summer (≈early flowering) PAI from 2009 (z_{0m} = 0.005*exp (2.42*PAI); p < 0.0001; n = 10), assuming that PAI = 0 corresponds to z_{0m} = 0.005, i.e., approximately z_{0m} for short grass [*Monteith and Unsworth*, 1990]. Using PAR_{albedo}, we calculated APAR with a simplified expression written as:

$$APAR = ((1 - PAR_{albedo}) - 0.05) * PAR \tag{4}$$

assuming a constant soil and grass background PAR_{albedo} of 0.05.

[23] Our basic assumption was that at the onset of flowering, i.e., on DOY_{flower}, daily PAR_{albedo} started to increase. For each year, we compared two periods of data: the 4 weeks (inclusive) prior and following DOY_{flower} + 10 days (allowing onset of flowering to be fully established, but starting before the canopy reaches its peak bloom). For each period, we gathered half-hourly F_A and PAR data where each data point in an eddy covariance time series represents an average of half-hour fluxes originated from within the footprint, i.e., the upwind source area of the eddy covariance system. The extent and orientation of the footprint depends on wind direction, measurement height, surface roughness, and atmospheric stability, and thus varies continuously over time. The data of $F_{A,norm}$-APAR (y ~ x in equation (1)) were divided into

blocks of 1 week (equal to 336 half hours). Each block was considered an independent realization (the subject i in equation (2)) of a temporal series of half-hourly $F_{A,norm}$ estimates at different APAR levels (index j in equation (2)). The temporal autocorrelation inherent in the measurements j (i.e., imposed diurnal cycles of APAR and thus $F_{A,norm}$) within each weekly data block (i.e., the associated correlation among the within-week errors of APAR and $F_{A,norm}$ measurements) was modeled as an autoregressive-moving average correlation model (ARMA [*Box et al.*, 1994]). Various correlation models were evaluated with normalized residual plots and subsequently compared sequentially with likelihood ratio tests and the Akaike Information Criterion as outlined by *Pinheiro and Bates* [2000]. With the final ARMA ($p = 1$, $q = 1$) correlation model, no significant autocorrelation at a significance level of 0.01 was observed.

[24] In contrast to canopy photosynthesis where an increase in leaf area translates directly into increased photosynthetic CO_2 uptake, F_{ER} is the sum of heterotrophic (F_{HR}) and autotrophic respiration (F_{AR}), which itself is often conceptualized as the sum of growth and maintenance respiration [*McCree*, 1970]. Growth respiration is associated with the production of new plant material, and thus photosynthetic CO_2 uptake, whereas maintenance respiration is associated with the preservation of existing plant material [*Amthor*, 2000]. It has been estimated that the contributions of the two autotrophic respiration components are about equal over the growing season [*Amthor*, 1984; *Sprugel*, 1990], but exceptions exist [e.g., *Paembonan et al.*, 1992]. Our second focus was on the effect of measurement year and flowering (2007 and 2009) and flowering/mowing (2008), respectively, on two model parameters (Q_{10} and F_{10}) of the following exponential temperature-response function (f in equation (2)):

$$F_{AR,norm} = F_{10,AR} * Q_{10,AR}^{(T_{air}-T_{10})/10} \quad (5)$$

where $F_{AR,norm}$ is F_{AR} normalized by PAI, $F_{10,AR}$ (μmol m^{-2} s^{-1}) is $F_{AR,norm}$ at a reference temperature of 10°C, and $Q_{10,AR}$ is the temperature sensitivity of $F_{AR,norm}$ to a 10°C temperature increase. Similar to $F_{A,norm}$, normalizing F_{AR} by PAI removed the effect of different amounts of respiring aboveground plant material between years ($F_{AR,norm}$).

[25] We calculated F_{AR} as the difference between F_{ER} and F_{HR}. We used weekly soil CO_2 efflux measured with a static chamber technique over bare soil in close proximity to the fenced enclosure as an approximation for weekly F_{HR} [*Teh et al.*, 2011]. Based on field observations, we assumed a 25% contribution from laterally spreading pepperweed roots that might have been present at the chamber measurement locations. First, we regressed soil CO_2 efflux (≈weekly F_{HR}) against accompanying weekly T_{soil} measurements made at the chamber measurement locations [*Teh et al.*, 2011] to quantify $Q_{10,HR}$ and $F_{10,HR}$ ($p < 0.0001$; $n = 28$) with equation (5). Next, we calculated half-hourly F_{HR} from the depth-integrated average T_{soil} (T_{soil_ave}; made within the fenced enclosure) with $Q_{10,HR}$ (=1.69) and $F_{10,HR}$ (=1.33 μmol m^{-2} s^{-1}), before calculating $F_{AR} = F_{ER} - F_{HR}$.

[26] Following the approach outlined above for APAR and $F_{A,norm}$, we extracted half-hourly F_{AR} and T_{air} data for the same two periods (preflowering and flowering). Again, after normalization of F_{AR} with PAI, each weekly $F_{AR,norm}$-T_{air} ($y \sim x$ in equation (1)) data block with half-hourly data pairs was treated as a series of repeated measurements at different T_{air} levels. Using the same diagnostics as for APAR and $F_{A,norm}$, the same ARMA($p = 1$, $q = 1$) correlation model as above was identified as suitable to capture the temporal autocorrelation inherent in the measurements within each week at a significance level of 0.01.

[27] We pursued a sequential model building approach to test changes and controls in the parameters governing equations (3) and (5), each consisting of six steps and resulting in models m1–m6: ignoring the week-based grouping by determining only one nonlinear least squares estimate of the parameters in equations (3) and (5) for the entire data set (m1), separate nonlinear least squares estimates of the parameters in equations (3) and (5) for each ($n = 24$) weekly data set (m2), treating each of the two variable parameters in equations (3) and (5) as mixed effects (β and u_i) in equation (2) with no covariates (m3), and finally sequentially incorporating different covariates in m3 (m4: measurement year; m5: flowering condition) and the interaction between measurement year and flowering condition in m3 (m6: measurement year and flowering condition). Our main criteria to assess the impact of flowering and mowing on $F_{A,norm}$ and F_{AR} was the random effect structure and the resulting required covariates on the fixed effects in equation (2) to explain the between-week variation in α and A_{max} (equation (3)) and $F_{10,AR}$ and $Q_{10,AR}$ (equation (5)) for different measurement years and flowering conditions in m3–m6. The differences in random effects were tested using Tukey-Kramer's honestly significant difference criterion. This criterion was also used to test the significance in the differences of seasonal totals of F_C, F_A and F_{ER} between unmowed (2007 and 2009) and mowed summers (2008). All analyses were done in the R computing environment (v.2.10.0 [*R Development Core Team*, 2010]).

3. Results

3.1. Seasonal Changes in Environmental Conditions and Net Ecosystem CO_2 Exchange

[28] The meteorological conditions in 2007–2009 on Sherman Island were characteristic for the Mediterranean climate of the Delta, i.e., hot summers and cool winters with almost all precipitation falling between October and April (Figure 1). Water table depth showed seasonal fluctuations of around 30 cm in response to precipitation input and reduced ET (data not shown) over the winter after which water table depth increased almost linearly with no further oscillations at our primary measurement site (Figure 1c).

[29] Based on field observations, we identified growth of pepperweed in late February (DOY 50), reaching a mean maximum PAI (standard deviation) of 0.85 (0.81) in mid-May (DOY 140) when plants were in peak bloom. The low mean PAI in combination with high standard deviation indicates the impact of grazing and trampling on structural canopy development, causing a discontinuous, open pepperweed canopy of varying height and density. Seasonal changes in daily z_{0m} were related to changes in plant growth and abundance (and thus PAI), reaching peaks in mid-May during early flowering (around DOY 140) when plants were fully grown (Figure 1d).

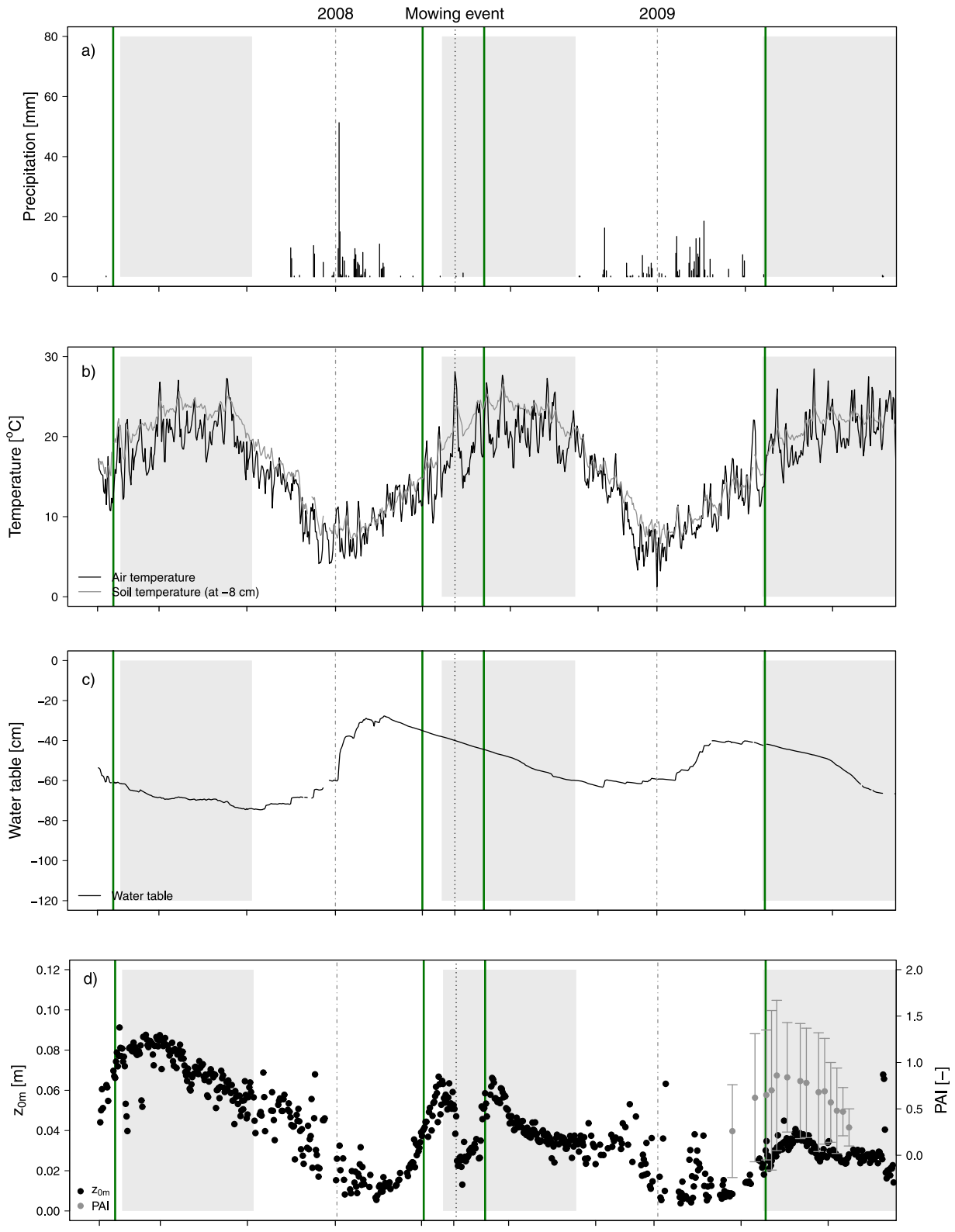

Figure 1. Seasonal changes in (a) daily total precipitation, daily mean (b) water table below the ground surface, (c) air and soil temperature, (d) plant area index (PAI) and surface roughness length (z_{0m}), (e) photosynthetically active radiation (PAR) and albedo of photosynthetically active radiation (PAR_{albedo}), (f) net ecosystem exchange (F_C) and canopy photosynthesis (F_A) and (g) ecosystem respiration (F_{ER}), separated into autotrophic respiration (F_{AR}) and heterotrophic respiration (F_{HR}). The gray shaded areas indicate the summers (1 May to 30 September) in 2007–2009; the dark green vertical lines indicate the onset of flowering in 2007–2009 based on increasing PAR_{albedo} (see text for further explanation).

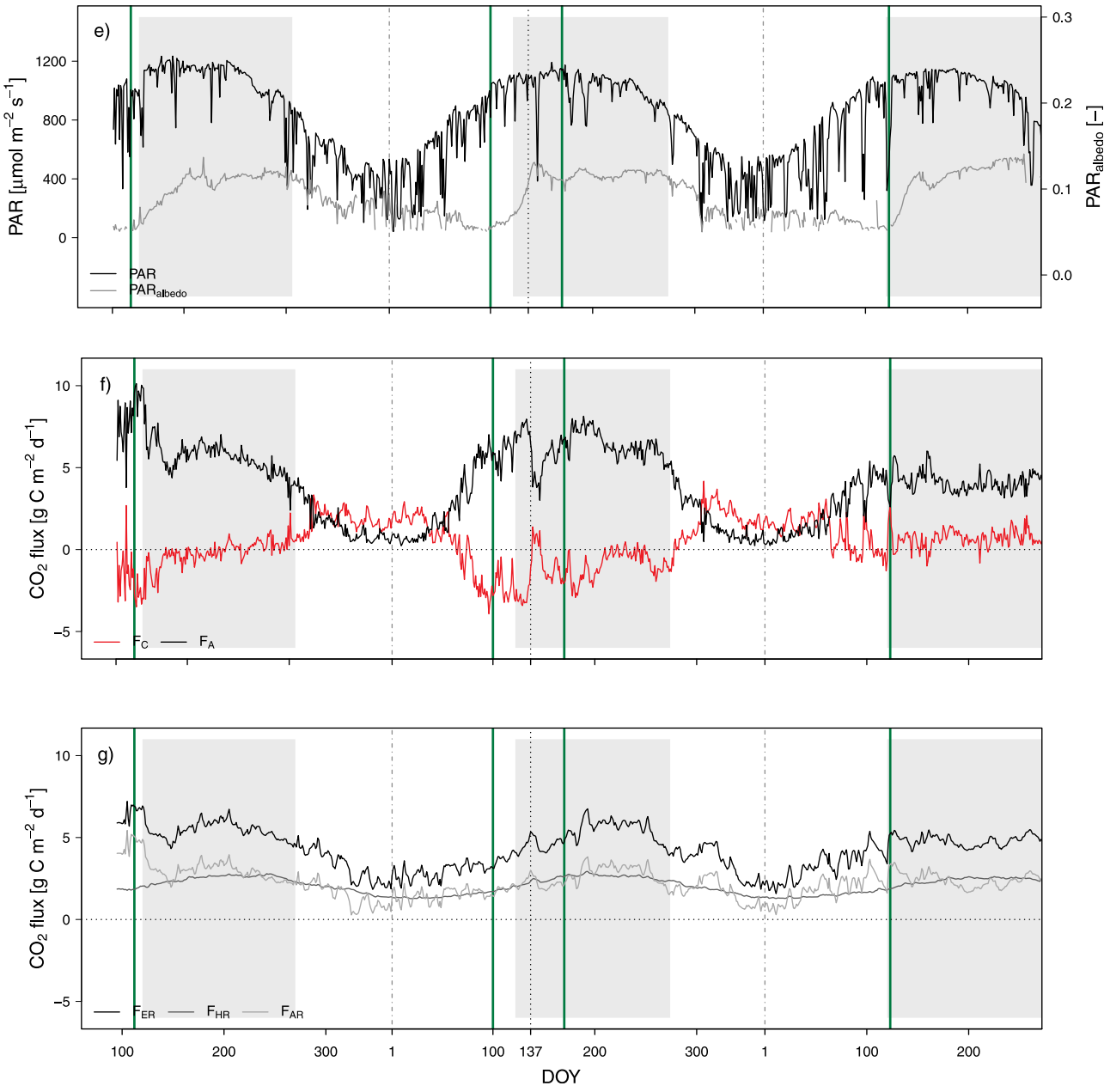

Figure 1. (continued)

[30] Daily variation of incoming PAR was related to cloudiness and other changes in atmospheric transmittance properties, and is regulated seasonally by the Earth's revolution (Figure 1e). Seasonal changes in PAR_{albedo} roughly coincided with pepperweed's key phenological phases: at the end of early vegetative growth, PAR_{albedo} started to rise with the onset of flowering, i.e., due to the increasing number of white flowers in late April/early May, until it reached a plateau with peak bloom throughout the flowering phase. Based on visual inspection of the PAR_{albedo} signal, we determined the onset of flowering as occurring on days 112, 100, 169 and 123 for cases in 2007, 2008 (premowing), 2008 (postmowing) and 2009, respectively (Figure 1e). In early October, PAR_{albedo} started to decrease during the seed maturation and senescence phases. Generally, the seasonal course of PAR_{albedo} was dominated by a spatially and temporally uniform first generation of plants. The mowing event during early flowering in 2008 caused PAR_{albedo} to first decrease and then increase again during pepperweed regrowth and the associated second flowering phase. Weekly to biweekly fluctuations in PAR_{albedo} were caused by the cooccurrence of various later generations of plants within the field of view of the downward looking quantum sensor. These later generations were at different development stages and together included green and senescent (brown) stems and leaves, and white flowers with bare soil or dead grass as

subcanopy background, together causing weekly to biweekly changes of the pepperweed canopy's spectral characteristics as tracked by PAR_{albedo}.

[31] Similar to PAR_{albedo}, F_C varied in correspondence to pepperweed's key phenological phases (Figure 1f). During germination and early vegetative growth, the pepperweed infestation showed increasing net CO_2 uptake, followed by an almost CO_2 neutral flowering phase. During and after senescence, the site was a net source of CO_2. Canopy photosynthesis increased continuously during early vegetative growth and eventually dropped before the canopy reached peak bloom (Figure 1f). In each year a minor peak in F_A was reached about 10–15 days prior to the main peak in F_A. There was a continuous decrease in maximum F_A over the study period from values around 10 (2007), over 8 (2008), to 6 g C m^{-2} d^{-1} (2009), indicating a decrease in pepperweed abundance with time. Due to the mowing event in 2008 (DOY 137), F_A dropped abruptly. Afterward, F_A increased as a result of immediate plant regrowth, before it declined again during the flowering phase of the postmowing pepperweed generation. Canopy photosynthesis then declined rapidly during senescence (~DOY 300). F_{ER} showed less pronounced seasonal fluctuations compared to F_A, but also responded with reductions due to flowering and to a lesser extent due to mowing (Figure 1g). F_{ER} increased during initial plant growth and regrowth after mowing. Our separation of F_{ER} into F_{HR} and F_{AR} suggests both components contributed about equally during the summer whereas the F_{AR} contribution was slightly increased (~0.5 g C m^{-2} d^{-1}) during early vegetative growth of pepperweed compared to F_{HR} and vice versa (~0.5 g C m^{-2} d^{-1}) during senescence toward the end of the year (Figure 1g).

3.2. Net Ecosystem CO_2 Exchange: Pepperweed Flowering and Mowing

[32] Our interest in the pepperweed infestation's F_A and F_{AR} focused on the combined effects and interactions of measurement year and flowering (2007 and 2009) and flowering/mowing (2008), respectively, toward the model parameters of the light (α; A_{max}: equation (3)) and temperature responses ($F_{10,AR}$; $Q_{10,AR}$: equation (5)), respectively. We assessed these interactions with the sequential application of nonlinear mixed-effects models (equation (2)).

[33] Initial scatterplots of the $F_{A,norm}$-APAR and $F_{AR,norm}$-T_{air} relationships conditioned into APAR and T_{air} bins, respectively, indicate that both measurement year and flowering condition affected $F_{A,norm}$ and F_{AR} in 2007–2009 (Figure 2): substantially higher $F_{A,norm}$ and $F_{AR,norm}$ for nonflowering pepperweed in 2007 and 2009 (both no mowing) but not in 2008 (mowing).

[34] Fitting one nonlinear (fixed effects) model to all half-hourly $F_{A,norm}$-APAR (equation (3)) and $F_{AR,norm}$-T_{air} (equation (5)) data neglects the variability introduced by measurement year and flowering condition (m1). As a result, the high residual standard errors for m1 and not the week-to-week parameter estimates (data not shown) reflect the effects of measurement year and flowering condition (Table 1).

[35] Explicit consideration of measurement year and flowering condition obtained through separate, week-to-week parameter estimates reduced the residual standard errors in m2 compared to m1 (Table 1). The α, A_{max}, $F_{10,AR}$ and $Q_{10,AR}$ estimates obtained from the separate fits in m2 suggest substantial between-week variation in α, A_{max} and $F_{10,AR}$ and to a lesser extent in $Q_{10,AR}$: no clear pattern emerges for α, which on average decreased for flowering pepperweed in 2007, remained almost constant in 2008, and then increased for flowering pepperweed in 2009 (Figure 3a). In contrast, on average A_{max} decreased for flowering pepperweed in 2007 and 2009, but not in 2008 when A_{max} was similar for flowering and nonflowering pepperweed (Figure 3b). On average $Q_{10,AR}$ increased slightly in 2007–2009 between nonflowering and flowering pepperweed (Figure 3c), while $F_{10,AR}$ decreased substantially for nonflowering pepperweed in 2007 and 2009 but increased in 2008 (Figure 3d). As a consequence of Figures 3a–3d, the inclusion of random effects for week-to-week estimates of all four parameters was justified to account for the between-week variation neglected in m1 (one overall estimate of α, A_{max}, $F_{10,AR}$ and $Q_{10,AR}$) and the overparameterization (24 separate estimates of α, A_{max}, $F_{10,AR}$ and $Q_{10,AR}$) through separate, week-to-week fits in m2.

[36] To identify the random effects structure for equations (3) and (5) in equation (2), we initially considered full models with each of the two parameters (α; A_{max}: equation (3) and $Q_{10,AR}$; $F_{10,AR}$: equation (5)) as mixed effects and no covariates on the fixed effects that might incorporate some of the variation accounted for through random effects (m3). Visual inspection of the standardized residuals plotted against the fitted values of m3 indicated homoscedastic within-week error variances (data not shown). Treating α, A_{max}, $Q_{10,AR}$ and $F_{10,AR}$ as mixed effects in m3 reduces the number of parameters required to capture between-week variation to one overall estimate of α, A_{max}, $F_{10,AR}$ and $Q_{10,AR}$, but had no impact on the reduced residual standard errors of m2 (Table 1). Weak negative correlations between α and A_{max} (correlation coefficient (r) = −0.10) and between $F_{10,AR}$ and $Q_{10,AR}$ (r = −0.38) suggests that equations (3) and (5) might be overparameterized in terms of random effects. We tested the need for random effects for all four parameters in m3 by considering random effects only for one of the parameters at a time: either for α or A_{max} (equation (3)), and either for $F_{10,AR}$ and $Q_{10,AR}$ (equation (5)). Subsequent comparison of these simplified models to the full models of m3 using likelihood ratio tests revealed that random effects were required for each of the two parameters in equations (3) and (5) ($p < 0.0001$).

[37] Visual inspection of the estimated random effects in m3 suggests the incorporation of measurement year and mowing condition as covariates on the fixed effects (Figure 4): on average no significant changes occurred in α in 2007–2009 but A_{max} decreased significantly for flowering pepperweed compared to nonflowering pepperweed by around 13 and 17 μmol m^{-2} s^{-1} in 2007 and in 2009, respectively (Table 2). There was no significant increase in A_{max} in 2008 between flowering and nonflowering pepperweed. Overall, $F_{10,AR}$ decreased significantly for flowering pepperweed compared to nonflowering pepperweed by almost 2 μmol m^{-2} s^{-1} in 2007 and 2009, respectively. Again, there was no significant increase in $F_{10,AR}$ in 2008 between flowering and nonflowering pepperweed. In 2007–2009, the random effects for $Q_{10,AR}$ were generally less variable for nonflowering than for flowering pepperweed. Similar to α, there was no significant

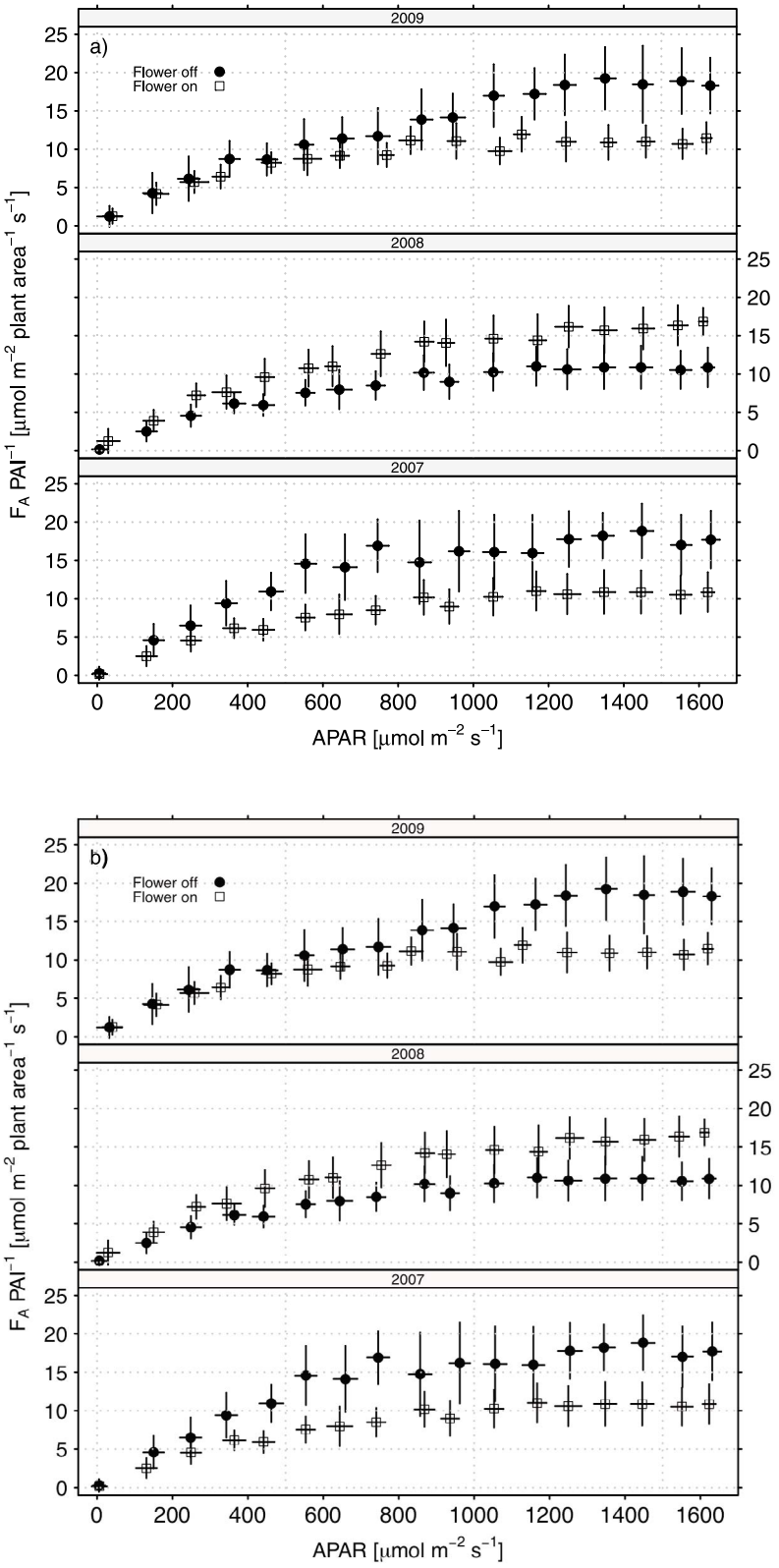

Figure 2. Conditional scatterplots for the nonlinear response of (a) canopy photosynthesis normalized by plant area index ($F_{A,norm}$: F_A PAI^{-1}) to absorbed photosynthetically active radiation (APAR) and of (b) autotrophic respiration normalized by PAI ($F_{AR,norm}$: F_{AR} PAI^{-1}) to air temperature (T_{air}). The $F_{A,norm}$-APAR data are binned in PAR-bins of 100 μmol m^{-2} s^{-1}, and the $F_{AR,norm}$-T_{air} data are binned in T_{air}-bins of 2°C. The vertical and horizontal lines through each bin data point indicate one standard deviation of F_A PAI^{-1} and F_{AR} PAI^{-1}, and APAR and T_{air}, respectively.

Table 1. Residual Standard Errors of Models m1–m6

	m1	m2	m3	m4	m5	m6
Canopy Photosynthesis: Light Response Curve (Equation (3))						
Residual SE[a] (μmol m^{-2} s^{-1})	3.07	2.11	2.14	2.14	2.14	2.13
Autotrophic Respiration: Temperature Response Curve (Equation (5))						
Residual SE (μmol m^{-2} s^{-1})	1.09	0.39	0.48	0.48	0.48	0.48

[a]SE, standard error.

pattern for $Q_{10,AR}$ related to measurement year or flowering condition. Overall, the different magnitudes in the changes of especially A_{max} in 2007 and 2009 suggest interacting covariates to explain the variability in the model parameters.

[38] We separately introduced measurement year (m4), flowering condition (m5), and finally measurement year, flowering condition and their interaction (m6) as covariates to explain the variation in α, A_{max}, $Q_{10,AR}$ and $F_{10,AR}$ in m3. The introduction of covariates in m4–m6 had no impact on the reduced residual standard errors of m2 compared to m1 (Table 1). Conditional *F* tests to test for the joint significance of the added fixed effects in m4–m6 (significances of individual fixed effects are not discussed) revealed that the added fixed effects in m4–m6 were either significant ($p < 0.01$; m5: α), highly significant ($p < 0.0001$; m4: $F_{10,AR}$, m5: A_{max}, $F_{10,AR}$; m6: A_{max}, $F_{10,AR}$) or not significant at a significance level of 0.01 (m4: α, A_{max}, $Q_{10,AR}$, m5: α, $Q_{10,AR}$, $F_{10,AR}$; m6: α, $Q_{10,AR}$), thus justifying the intro-

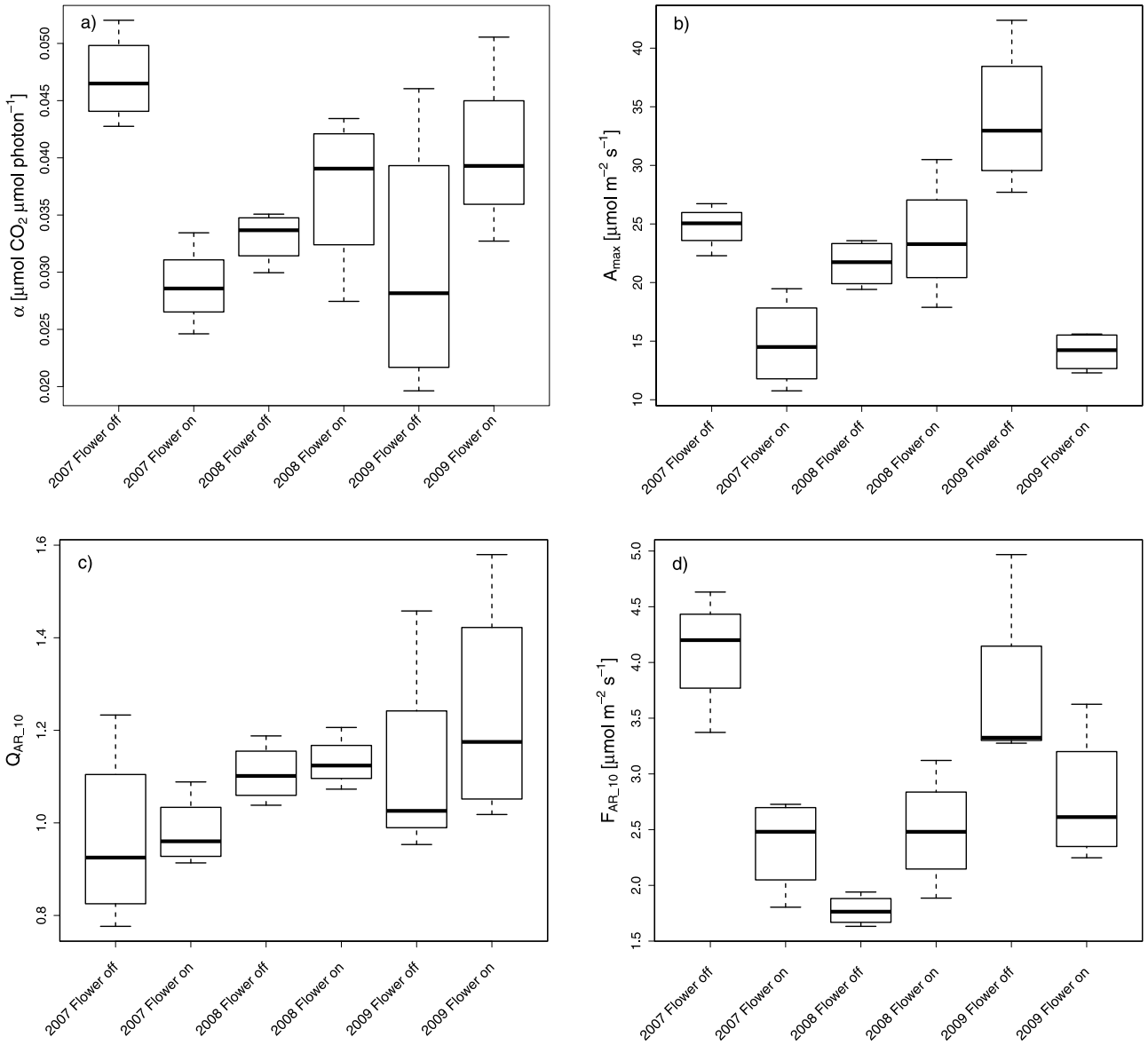

Figure 3. Boxplots of parameter estimates obtained from separate, week-to-week fits to equations (3) and (5) (m2): (a) effective quantum yield (α), (b) maximum photosynthetic capacity (A_{max}), (c) autotrophic respiration at a reference temperature of 10°C (F_{AR_10}), and (d) temperature sensitivity of F_{AR_10} to a 10°C temperature increase (Q_{10_AR}). "Flower off" and "Flower on" denote nonflowering and flowering pepperweed, respectively.

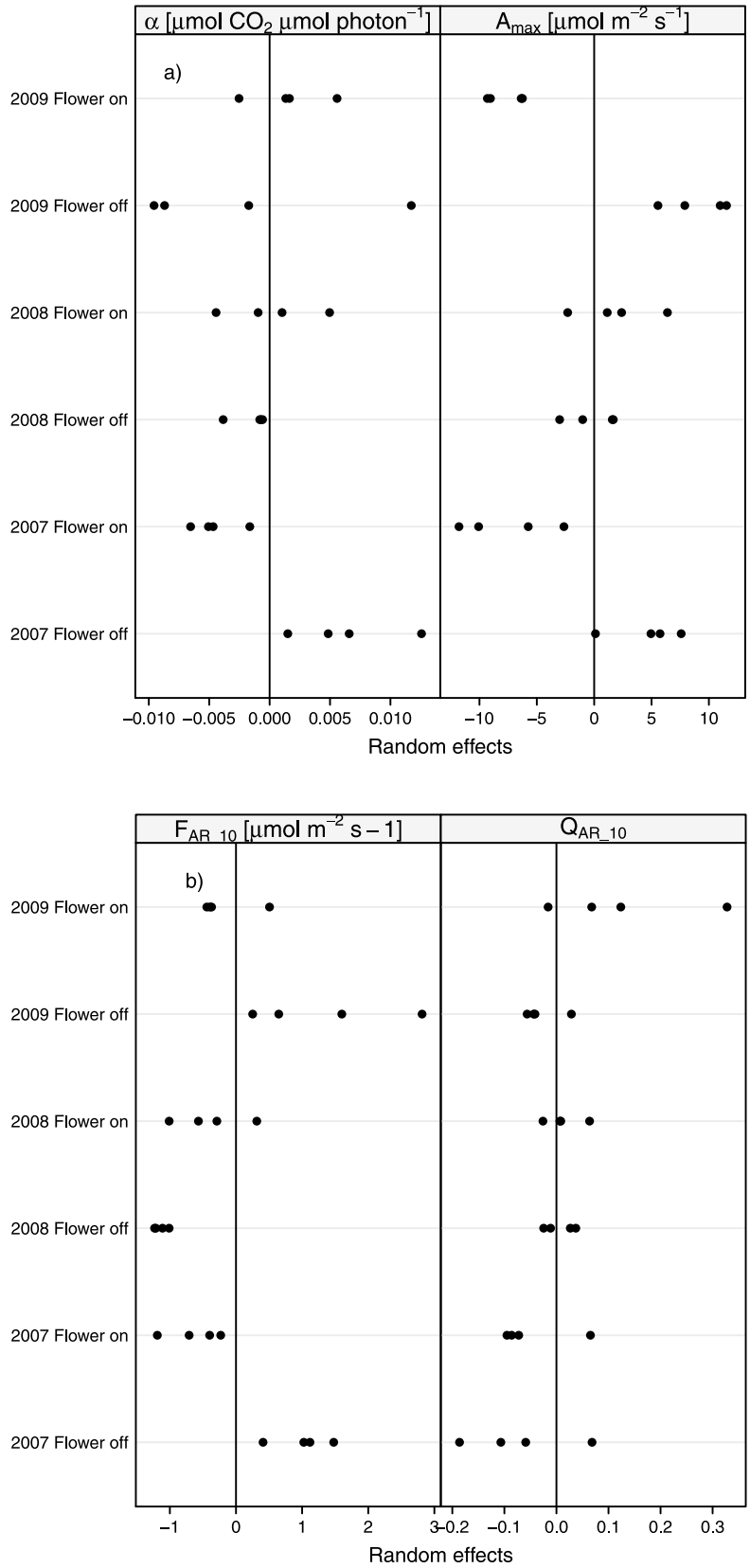

Figure 4. Random effects structure for (a) equation (3) and (b) equation (5) in equation (2) with each of the two parameters α and A_{max} (Figure 4a), and F_{AR_10} and Q_{10_AR} (Figure 4b), as mixed effects and no covariates on the fixed effects (m3). "Flower off" and "Flower on" denote nonflowering and flowering pepperweed, respectively. Each point represents one weekly data block.

Table 2. Mean (Standard Error) Random Effects of Mixed-Effects Models m3[a]

	2007		2008		2009	
	Flower off	Flower on	Flower off	Flower on	Flower off	Flower on
Canopy Photosynthesis: Light Response Curve (Equation (3))						
α (μmol CO_2 μmol photon^{-1})	0.006 (a) (0.002)	−0.004 (a) (0.001)	−0.001 (a) (0.001)	0.001 (a) (0.002)	−0.002 (a) (0.005)	0.002 (a) (0.002)
A_{max} (μmol m^{-2} s^{-1})	4.58 (ab) (1.59)	−8.52 (c) (1.73)	−0.19 (b) (1.12)	1.90 (b) (1.80)	9.00 (a) (1.40)	−7.74 (c) (0.83)
Autotrophic Respiration: Temperature Response Curve (Equation (5))						
$F_{AR,10}$ (μmol m^{-2} s^{-1})	1.00 (ab) (0.22)	−0.63 (c) (0.21)	−1.14 (c) (0.05)	−0.39 (c) (0.28)	1.33 (a) (0.57)	−0.18 (bc) (0.23)
$Q_{10,AR}$	−0.07 (b) (0.05)	−0.05 (ab) (0.04)	0.01 (ab) (0.01)	0.01 (ab) (0.02)	−0.03 (ab) (0.02)	0.12 (a) (0.07)

[a]Different letters in parentheses indicate differences in the four parameters of equations (3) and (5) at a significance level of 0.05 (Tukey-Kramer's honestly significant difference criterion).

duction of covariates for at least A_{max} and $F_{10,AR}$. Incorporation of fixed effects through m4–m6 caused a reduction in the standard deviations of A_{max} and $F_{10,AR}$ compared to the models of m3 (Table 3). We tested if the models of m6 still required random effects after the introduction of interacting covariates by separately eliminating random effects and subsequent model comparison using likelihood ratio tests. All model comparisons were significant at a significance level of 0.01, indicating that random effects were still required in m6 (even for $Q_{10,AR}$) in addition to interacting covariates to explain the variability in α, A_{max}, $Q_{10,AR}$ and $F_{10,AR}$. However, in contrast to m3 (Figure 4), the random effects of m6 did not show a systematic pattern (data not shown).

3.3. Summer Net Ecosystem CO_2 Exchange

[39] The mowing event in 2008 (DOY 137) caused an abrupt decrease in F_A followed by increased CO_2 uptake during immediate pepperweed regrowth, while F_{ER} responded similarly but with a less pronounced change (Figure 1e). As expected, the mowing event is also reflected in the summer period totals (Figure 5). Both total F_A and F_{ER} were highest for the 2008 summer period, when the pepperweed infestation acted as a moderate sink with respect to CO_2 (−174 g C m^{-2} period^{-1}). In contrast, the site was almost CO_2 neutral (−28 g C m^{-2} period^{-1}) for the 2007 summer period, and even acted as a CO_2 source (129 g C m^{-2} period^{-1}) for the 2009 summer period. Taking into account the uncertainty due to gap-filling, mean summer totals of F_C, F_A and F_{ER} were all significantly different among the 3 years.

4. Discussion

[40] Pepperweed's most prominent key phenological phase is flowering when the canopy contains a dense arrangement of small white flowers. Quantifying the effect of flowering on canopy F_A and F_{ER} is a major challenge. We quantified the effect of pepperweed flowering on both component fluxes through nonlinear mixed-effects models (equation (2)) formulated for the responses of $F_{A,norm}$ to light (i.e., APAR; equation (3)) and of $F_{AR,norm}$ to temperature (i.e., T_{air}, equation (5)). The obtained estimates for A_{max} (equation (3)) and $F_{10,AR}$ (equation (5)) were influenced by measurement year and flowering condition, especially in 2007 and 2009 (Figure 4). Both A_{max} and $F_{10,AR}$ decreased in response to flowering but at different magnitudes (quantified as the difference in random effects between flowering and non-flowering pepperweed in m3; Table 2). In contrast, these two variable parameters did not change significantly in 2008 according to flowering condition, which we interpret as the result of mowing and immediate pepperweed regrowth (Table 2). Step by step, measurement year (m4) and flowering condition (m5) were incorporated as interacting covariates (m6) on the fixed effects in equation (2), thus highlighting

Table 3. Standard Deviation of Random Effects and Fixed Effects of Mixed Effects Models m3–m6[a]

	m3	m4	m5	m6
Canopy Photosynthesis: Light Response Curve (Equation (3))				
Random effects				
A (SD)	0.007	0.006	0.007	0.005
A_{max} (SD)	6.90	6.80	5.04	2.89
Autotrophic Respiration: Temperature Response Curve (Equation (5))				
Random effects				
$Q_{10,AR}$ (SD)	0.10	0.07	0.09	0.07
$F_{AR,10}$ (SD)	1.06	0.87	0.97	0.48
Canopy Photosynthesis: Light-Response Curve (Equation (3))				
Fixed effects				
α (SE)	0.033 (0.002)	0.033 (0.002)	0.033 (0.002)	0.033 (0.002)
A_{max} (SE)	22.65 (1.47)	22.65 (1.45)	22.67 (1.11)	22.97 (0.66)
Autotrophic Respiration: Temperature-Response Curve (Equation (5))				
Fixed effects				
$F_{AR,10}$ (SE)	3.07 (0.22)	3.06 (0.18)	3.06 (0.20)	3.06 (0.11)
$Q_{10,AR}$ (SE)	1.04 (0.02)	1.04 (0.02)	1.04 (0.02)	1.04 (0.02)

[a]Units are the same as in Table 2. SD, standard deviation; SE, standard error.

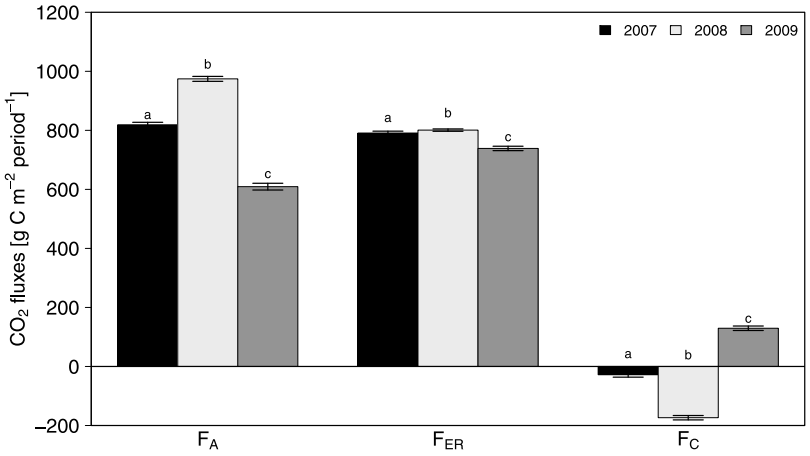

Figure 5. Mean summer (1 May to 30 September) totals of net ecosystem CO_2 exchange (F_C), canopy photosynthesis (F_A), and ecosystem respiration (F_{ER}) for 100 data sets using a bootstrapping technique. Uncertainties due to gap filling are reported as one standard deviation. Different letters indicate the totals are significantly different at a significance level of 0.05 (Tukey-Kramer's honestly significant difference criterion).

the importance of these two factors for explaining some of the variation in A_{max} and $F_{10,AR}$ previously explained by random effects alone (m3).

[41] Based on our results, the question arises of how the reduction in especially F_A relates to pepperweed's success as an invasive plant. We assume that the combination of other functional traits such as the plant's aggressive vegetative growth, deep rhizome penetration, and prolific bud production and reproduction by seeds [*Francis and Warwick*, 2007] is in the long term of greater relevance for pepperweed's success as an invasive plant than a short-term (i.e., several months) reduction in photosynthetic CO_2 uptake.

[42] Pepperweed regrowth after mowing in 2008 caused the pasture to be a moderate net summer sink for CO_2 in 2008 instead of being almost neutral (2007) or a small source (2009) with respect to CO_2. Because of the timing of the mowing event, i.e., during early flowering, the duration of the vegetative growth phase was prolonged relative to 2007 and 2009 over late spring/early summer when PAR was at maximum and the regrowing plants were the most productive. Considering the seasonal course of PAR (Figure 1e), it can be assumed that mowing later during flowering or even during seed maturation, the reversal of the attenuating effects of flowering by pepperweed regrowing under lower PAR levels would have been minimized. Thus, from a CO_2 balance perspective, it appears that the timing of the mowing was at or close to optimum. However, to assess the long-term effectiveness of the mowing event and its timing, and to better understand the link between pepperweed phenology, applied control measure and infestation dynamics [*Wolkovich and Cleland*, 2010], analysis of multiple years of premowing and postmowing F_C measurements from pepperweed infested and uninfested sites would be required.

[43] The site was subjected to year-round grazing causing a discontinuous, open pepperweed canopy of varying density, relatively low height and consequently low PAI. Thus, we assume that sufficient light was able to penetrate even to the lowest leaves in the peppweed canopy and that decreased F_A in response to pepperweed flowering was not simply caused by APAR limitation due to shading of leaves underneath a closed canopy top of dense flowers. Unfortunately, we cannot provide estimates for the amount of light that reached the lower leaves of the pepperweed infestation.

[44] Very little is known about the impact of flowering on photosynthesis in general [*Urban et al.*, 2008], and our ecosystem-scale measurement of F_C prevents a thorough mechanistic explanation of the observed decrease in pepperweed F_A and F_{AR} due to flowering. There is some evidence for flowering-related decreases in photosynthetic CO_2 uptake reported in the literature [e.g., *Shivashankara and Mahai*, 2000; *Urban et al.*, 2008], and several ideas are discussed that might provide an explanation for our findings. One of the most thorough analyses was provided by *Urban et al.* [2008] who attributed decreased net photosynthetic CO_2 uptake in flowering mango (*Mangifera indica* L.) to decreases in stomatal and mesophyll conductances and reduced photosynthetic capacity as indicated by the light-saturated rate of photosynthetic electron transport due to decreased leaf N content. Decreased pepperweed leaf N content roughly coincides with our observed drop in F_A due to flowering just before the mowing event in 2008 [*Runkle*, 2009].

[45] The same author reports results from leaf-level cuvette chamber measurements made with a portable steady state photosynthetic measurement system (LI-6400; LI-COR; with attached fluorescence chamber head to modify light levels) on leaves of randomly selected pepperweed plants in 2008 [*Runkle*, 2009]. Leaf-level photosynthetic response of pepperweed to light was determined with equation (3) (with an additional term for respiration at zero irradiance). Values of A_{max} derived by this method had little detectable change based on flowering condition, and have a mean value of 38.7 μmol m^{-2} s^{-1} for leaves of both preflowering (n = 2) and flowering plants (n = 7). Mean values for α were 0.047 μmol CO_2 μmol $photon^{-1}$ and 0.046 μmol CO_2 μmol $photon^{-1}$ for leaves of preflowering and flowering plants, respectively. Mean daytime respiration in the dark determined at the leaf level was 4.88 μmol m^{-2} s^{-1} in leaves of preflowering plants and 2.17 μmol m^{-2} s^{-1} in leaves of

flowering plants. However, considering the small sample size and sporadic nature of these leaf-level measurements, a direct comparison with our ecosystem-scale estimates is informative but inconclusive. Most likely other variables such as temperature, nutrition and time of day acted as stronger controls on A_{max}, α and R_d than flowering condition for specific leaves.

[46] Considering the close coupling between F_A and the growth respiration component of F_{AR}, we speculate that overall F_{ER} roughly followed the trend in F_A, albeit in a much less pronounced manner due to different plant physiological and environmental controls over the contributions by the maintenance respiration component of F_{AR} and by F_{HR} to F_{ER}. Most likely, two additional factors were important for the contribution by F_{HR} to F_{ER}. First, the presence of cattle over the entire study period contributed to mulching the soil surface with trampled pepperweed including vertical senesced plants from previous growing seasons, consequently accelerating plant decomposition. Since mowed pepperweed was left on the ground surface and not removed from the pasture, accelerated decomposition of trampled pepperweed litter might have been a major contributor F_{ER} after the mowing event. Second, F_{HR} at the pasture is in part driven by peat oxidation [*Deverel and Rojstaczer*, 1996], which is decoupled from the occurrence of pepperweed.

5. Conclusions

[47] For this study we analyzed CO_2 flux measurements spanning three growing seasons from a pepperweed-infested pasture in California with the goal of exploring the link between pepperweed flowering, mowing and F_C. We found that pepperweed flowering substantially reduced photosynthethic CO_2 uptake due to reduced maximum photosynthetic capacity during the plant's prime photosynthetic period. Similarly, flowering reduced autotrophic respiration, F_{AR}, and thus ecosystem respiration, F_{ER}, most likely because of reduced growth respiration as a function of reduced canopy photosynthesis, F_A. The reduction in F_{AR} in response to flowering was much less pronounced than for F_A. In contrast, the attenuating impacts of flowering on F_A and F_{AR} and thus F_{ER} were eliminated by pepperweed regrowing after mowing at the optimal time (from a CO_2 balance perspective), i.e., during early flowering. Our study is an example for the tight link between an invasive plant's prominent key phenological phase and applied control measures: a single mowing event at around the optimal time, i.e., early during flowering, has the potential to change the sign of the infestation's CO_2 source-sink strength.

[48] **Acknowledgments.** We thank Rodrigo Vargas, Youngryel Ryu (both University of California, Berkeley), and Matthias Peichl (University College Cork) for fruitful discussions during the preparation of the manuscript. We also thank Ted Hehn and Joseph Verfaillie for their dedicated support in conducting the field measurements and servicing the instruments. We thank the Editor, Timothy Griffis, and the two anonymous reviewers for their constructive comments that substantially improved the manuscript. This study was funded by National Science Foundation grant 0628720.

References

Amthor, J. S. (1984), The role of maintenance respiration in plant growth, *Plant Cell Environ.*, *7*, 561–569.

Amthor, J. S. (2000), The McCree-de Witt-Penning de Vries-Thornley respiration paradigms: 30 years later, *Ann. Bot.*, *86*, 1–20, doi:10.1006/anbo.2000.1175.

Andrew, M. E., and S. L. Ustin (2006), Spectral and physiological uniqueness of perennial pepperweed (*Lepidium latifolium*), *Weed Sci.*, *54*, 1051–1062, doi:10.1614/WS-06-063R1.1.

Andrew, M. E., and S. L. Ustin (2008), The role of environmental context in mapping invasive plants with hyperspectral image data, *Remote Sens. Environ.*, *112*, 4301–4317, doi:10.1016/j.rse.2008.07.016.

Baldocchi, D. D. (2003), Assessing the eddy covariance technique for evaluating carbon dioxide exchange rates of ecosystems: Past, present and future, *Global Change Biol.*, *9*, 479–492, doi:10.1046/j.1365-2486.2003.00629.x.

Baldocchi, D. D. (2008), Breathing of the terrestrial biosphere: Lessons learned from a global network of carbon dioxide flux measurement systems, *Aust. J. Bot.*, *56*, 1–26, doi:10.1071/BT07151.

Bergeron, O., A. M. Margolis, T. A. Black, C. Coursolle, A. L. Dunn, A. G. Barr, and S. C. Wofsy (2007), Comparison of carbon dioxide fluxes over three boreal black spruce forests in Canada, *Global Change Biol.*, *13*, 89–107, doi:10.1111/j.1365-2486.2006.01281.x.

Blank, R. R., and J. A. Young (2004), Influence of three weed species on soil nutrient dynamics, *Soil Sci.*, *169*, 385–397, doi:10.1097/01.ss.0000128013.15268.17.

Box, G. E. P., G. M. Jenkins, and G. C. Reinsel (1994), *Time Series Analysis: Forecastig and Control*, 3rd ed., Holden-Day, San Francisco, Calif.

Chen, J. M. (1996), Optically based methods for measuring seasonal variation in leaf area index of boreal conifer stands, *Agric. For. Meteorol.*, *80*, 135–163, doi:10.1016/0168-1923(95)02291-0.

D'Antonio, C. M., and P. M. Vitousek (1992), Biological invasions by exotic grasses, the grass fire cycle, and global change, *Annu. Rev. Ecol. Syst.*, *23*, 63–87.

Davidian, M., and D. M. Giltinan (2003), Nonlinear models for repeated measurement data: An overview and update, *J. Agric. Biol. Environ. Stat.*, *8*, 387–419, doi:10.1198/1085711032697.

Detto, M., and G. G. Katul (2007), Simplified expressions for adjusting higher-order turbulent statistics obtained from open path gas analyzers, *Boundary Layer Meteorol.*, *122*, 205–216, doi:10.1007/s10546-006-9105-1.

Detto, M., D. D. Baldocchi, and G. G. Katul (2010), Scaling properties of biologically active scalar concentration fluctuations in the surface boundary layer over a managed peatland, *Boundary Layer Meteorol.*, *136*, 407–430, doi:10.1007/s10546-010-9514-z.

Deverel, S. J., and S. Rojstaczer (1996), Subsidence of agricultural lands in the Sacramento San Joaquin Delta, California: Role of aqueous and gaseous carbon fluxes, *Water Resour. Res.*, *32*, 2359–2367, doi:10.1029/96WR01338.

Deverel, S. J., D. A. Leighton, and M. R. Finlay (2007), Processes affecting agricultural drainwater quality and organic carbon load in California's Sacramento–San Joaquin Delta, *San Francisco Estuary Watershed Sci.*, *5*(2).

Drenovsky, R. E., C. E. Martin, M. R. Falasco, and J. J. James (2008), Variation in resource acquisition and utilization traits between native and invasive perennial forbs, *Am. J. Bot.*, *95*, 681–687, doi:10.3732/ajb.2007408.

Drexler, J. Z., C. S. de Fontaine, and S. J. Deverel (2009), The legacy of wetland drainage on the remaining peat in the Sacramento-San Joaquin Delta, California, USA, *Wetlands*, *29*, 372–386, doi:10.1672/08-97.1.

Ehrenfeld, J. G. (2003), Effects of exotic plant invasions on soil nutrient cycling processes, *Ecosystems*, *6*, 503–523, doi:10.1007/s10021-002-0151-3.

Francis, A., and S. I. Warwick (2007), The biology of invasive alien plants in Canada. 8. *Lepidium latifolium* L, Can. *J. Plant Sci.*, *87*, 639–658.

Funk, J. L., and P. M. Vitousek (2007), Resource-use efficiency and plant invasion in low-resource systems, *Nature*, *446*, 1079–1081, doi:10.1038/nature05719.

Garratt, J. R. (1992), *The Atmospheric Boundary Layer*, Cambridge Univ. Press, New York.

Godoy, O., D. M. Richardson, F. Valladares, and P. Castro-Diez (2009), Flowering phenology of invasive alien plant species compared with native species in three Mediterranean-type ecosystems, *Ann. Bot.*, *103*, 485–494, doi:10.1093/aob/mcn232.

Healey, M. C. (2008), Science and the Bay-Delta, in *The State of Bay-Delta Science*, edited by M. C. Healey, M. D. Dettinger, and R. B. Norgaard, pp. 19–36, CALFED Sci. Program, Sacramento, Calif.

Humphreys, E. R., P. M. Lafleur, L. B. Flanagan, N. Hedstrom, K. H. Syed, A. J. Glenn, and R. Granger (2006), Summer carbon dioxide and water vapor fluxes across a range of northern peatlands, *J. Geophys. Res.*, *111*, G04011, doi:10.1029/2005JG000111.

Hunt, J. E., F. M. Kelliher, T. M. McSeveny, and J. N. Byers (2002), Evaporation and carbon dioxide exchange between the atmosphere and a

tussock grassland during a summer drought, *Agric. For. Meteorol.*, *111*, 65–82, doi:10.1016/S0168-1923(02)00006-0.

Kaimal, J. C., and J. E. Gaynor (1991), Another look at sonic thermometry, *Boundary Layer Meteorol.*, *56*, 401–410, doi:10.1007/BF00119215.

Koteen, L. (2009), A comparison of carbon cycling between native perennial and non-native annual grass communities in northern coastal California, Ph.D. thesis, Univ. of Calif., Berkeley.

Lasslop, G., M. Reichstein, D. Papale, A. D. Richardson, A. Arneth, A. Barr, P. Stoy, and G. Wohlfahrt (2010), Separation of net ecosystem exchange into assimilation and respiration using a light response curve approach: Critical issues and global evaluation, *Global Change Biol.*, *16*, 187–208, doi:10.1111/j.1365-2486.2009.02041.x.

Lin, S. T., B. T. Guan, and T. Y. Chang (2008), Fitting photosynthetic irradiance response curves with nonlinear mixed-effects models, *Taiwan J. For. Sci.*, *23*, 55–69.

Lindroth, A. (1993), Aerodynamic and canopy resistance of short-rotation forest in relation to leaf area index and climate, *Boundary Layer Meteorol.*, *66*, 265–279, doi:10.1007/BF00705478.

Lindstrom, M. J., and D. M. Bates (1990), Nonlinear mixed-effects models for repeated measures data, *Biometrics*, *46*, 673–687, doi:10.2307/2532087.

Mack, R. N., D. Simberloff, W. M. Lonsdale, H. Evans, M. Clout, and F. A. Bazzaz (2000), Biotic invasions: Causes, epidemiology, global consequences, and control, *Ecol. Appl.*, *10*, 689–710, doi:10.1890/1051-0761(2000)010[0689:BICEGC]2.0.CO;2.

McCree, K. J. (1970), Equations for the rate of respiration of white clover plants grown under controlled conditions, in *Prediction and Measurement of Photosynthetic Productivity*, edited by I. Setlik, pp. 221–229, Cent. for Agric. Publ. and Doc., Wageningen, Netherlands.

Monteith, J. L., and M. H. Unsworth (1990), *Principles of Environmental Physics*, Edward Arnold, London.

Mount, J., and R. Twiss (2005), Subsidence, sea level rise and seismicity in the Sacramento–San Joaquin Delta, *San Francisco Estuary Watershed Sci.*, *3*(1).

Ostertag, R., S. Cordell, J. Michaud, T. C. Cole, J. R. Schulten, K. M. Publico, and J. H. Enoka (2009), Ecosystem and restoration consequences of invasive woody species removal in Hawaiian Lowland wet forest, *Ecosystems*, *12*, 503–515, doi:10.1007/s10021-009-9239-3.

Paembonan, S. A., A. Hagihara, and K. Hozumi (1992), Long-term respiration in relation to growth and maintenance processes of the aboveground parts of hinoki forest tree, *Tree Physiol.*, *10*, 101–110.

Papale, D., and R. Valentini (2003), A new assessment of European forests carbon exchanges by eddy fluxes and artificial neuronal network spatialization, *Global Change Biol.*, *9*, 525–535, doi:10.1046/j.1365-2486.2003.00609.x.

Peek, M. S., E. Russek-Cohen, D. A. Wait, and I. N. Forseth (2002), Physiological response curve analysis using nonlinear mixed models, *Oecologia*, *132*, 175–180, doi:10.1007/s00442-002-0954-0.

Pinheiro, J. C., and D. M. Bates (2000), *Mixed-Effects Models in S and S-Plus*, Springer, New York.

Potts, D. L., W. S. Harpole, M. L. Goulden, and K. N. Suding (2008), The impact of invasion and subsequent removal of an exotic thistle, Cynara cardunculus, on CO_2 and H_2O vapor exchange in a coastal California grassland, *Biol. Invasions*, *10*, 1073–1084, doi:10.1007/s10530-007-9185-y.

Prater, M. R., D. Obrist, J. A. Arnone, and E. H. DeLucia (2006), Net carbon exchange and evapotranspiration in postfire and intact sagebrush communities in the Great Basin, *Oecologia*, *146*, 595–607, doi:10.1007/s00442-005-0231-0.

Raupach, M. R. (1994), Simplified expression for vegetation roughness length and zero-displacement as functions of canopy height and area index, *Boundary Layer Meteorol.*, *71*, 211–216, doi:10.1007/BF00709229.

R Development Core Team (2010), R: A language and environment for statistical computing, R Found. for Stat. Comput., Vienna. (Available at http://www.R-project.org)

Reichard, S. H., and C. W. Hamilton (1997), Predicting invasions of woody plants introduced into North America, *Conserv. Biol.*, *11*, 193–203, doi:10.1046/j.1523-1739.1997.95473.x.

Renz, M. J., and R. R. Blank (2004), Influence of perennial pepperweed (*Lepidium latifolium* L.) biology and plant-soil relationships on management and restoration, *Weed Technol.*, *18*, 1359–1363, doi:10.1614/0890-037X(2004)018[1359:IOPPLL]2.0.CO;2.

Runkle, B. R. K. (2009), Plant water use and growth in response to soil salinity in irrigated agriculture, Ph.D. thesis, Univ. of Calif., Berkeley.

Ryu, Y., T. Nilson, H. Kobayashi, O. Sonnentag, B. E. Law, and D. D. Baldocchi (2010), On the correct estimation of effective leaf area index: Does it reveal information on clumping effects?, *Agric. For. Meteorol.*, *150*, 463–472, doi:10.1016/j.agrformet.2010.01.009.

Schotanus, P., F. T. M. Nieuwstadt, and H. A. R. DeBruin (1983), Temperature measurement with a sonic anemometer and its application to heat and moisture fluctuations, *Boundary Layer Meteorol.*, *26*, 81–93, doi:10.1007/BF00164332.

Shaw, R. H., and A. R. Pereira (1982), Aerodynamic roughness of a plant canopy: A numerical experiment, *Agric. Meteorol.*, *26*, 51–65, doi:10.1016/0002-1571(82)90057-7.

Shivashankara, K. S., and C. K. Mahai (2000), Inhibition of photosynthesis by flowering in mango (*Mangifera Indica* L.), *Sci. Hortic.*, *83*, 205–212, doi:10.1016/S0304-4238(99)00085-0.

Sonnentag, O., J. Talbot, N. T. Roulet, and J. M. Chen (2007), Using direct and indirect measurements of leaf area index to characterize the shrub canopy of ombrotrophic peatland, *Agric. For. Meteorol.*, *144*, 200–212, doi:10.1016/j.agrformet.2007.03.001.

Sonnentag, O., G. van der Kamp, A. G. Barr, and J. M. Chen (2010), On the relationship between water table depth and water vapor and carbon dioxide fluxes in a minerotrophic fen, *Global Change Biol.*, *16*, 1762–1776, doi:10.1111/j.1365-2486.2009.02032.x.

Sprugel, D. G. (1990), Components of woody-tissue respiration in young *Abies amabilis* (Dougl.) Forbes trees, *Trees*, *4*, 88–98, doi:10.1007/BF00226071.

Tanner, C. B., and G. W. Thurtell (1969), Anemoclinometer measurements of Reynold stress and heat transport in the atmospheric surface layer, *U.S. Army Electron. Command Tech. Rep. ECOM 66–G22-F*, Univ. of Wis., Madison.

Teh, Y. A., W. L. Silver, O. Sonnentag, M. Detto, M. Kelly, and D. D. Baldocchi (2011), Large greenhouse gas emissions from a temperate peatland pasture, *Ecosystems*, doi:10.1007/s10021-011-9411-4, in press.

Urban, L., L. Jegouzo, and G. Damour (2008), Interpreting the decrease in leaf photosynthesis during flowering in mango, *Tree Physiol.*, *28*, 1025–1036.

Webb, E. K., G. I. Pearman, and R. Leuning (1980), Correction of flux measurements for density effects due to heat and water vapor transfer, *Q. J. R. Meteorol. Soc.*, *106*, 85–100, doi:10.1002/qj.49710644707.

Welles, J. M., and J. M. Norman (1991), Instrument for indirect measurement of canopy architecture, *Agron. J.*, *83*, 818–825, doi:10.2134/agronj1991.00021962008300050009x.

Wilson, K., et al. (2002), Energy balance closure at FLUXNET sites, *Agric. For. Meteorol.*, *113*, 223–243, doi:10.1016/S0168-1923(02)00109-0.

Wolkovich, E. M., and E. C. Cleland (2010), The phenology of plant invasions: A community ecology perspective, *Front. Ecol. Environ*, doi:10.1890/100033.

Young, J. A., D. E. Palmquist, and R. R. Blank (1998), The ecology and control of perennial pepperweed (*Lepidium latifolium* L.), *Weed Technol.*, *12*, 402–405.

D. D. Baldocchi, M. Detto, M. Kelly, W. L. Silver, O. Sonnentag, and Y. A. Teh, Department of Environmental Science, Policy, and Management, University of California, 137 Mulford Hall #3115, Berkeley, CA 94720, USA. (oliver.sonnentag@gmail.com)

B. R. K. Runkle, Department of Soil Science, University of Hamburg, Allende-Platz 2, D-20146 Hamburg, Germany.